REPORT

Accelerated multiphase water transformation in global mountain regions since 1990

Zongxing Li,[1,2] Qi Feng,[1,2] Xufeng Wang,[1,2] Zongjie Li,[3,*] Q J Wang,[4] Deliang Chen,[5,*] Baijuan Zhang,[1,2] and Juan Gui[1,2]

*Correspondence: lzjie314@163.com (Z.L.); deliang@gvc.gu.se (D.C.)

Received: July 15, 2023; Accepted: November 8, 2023; Published Online: November 15, 2023; https://doi.org/10.59717/j.xinn-geo.2023.100033

GRAPHICAL ABSTRACT

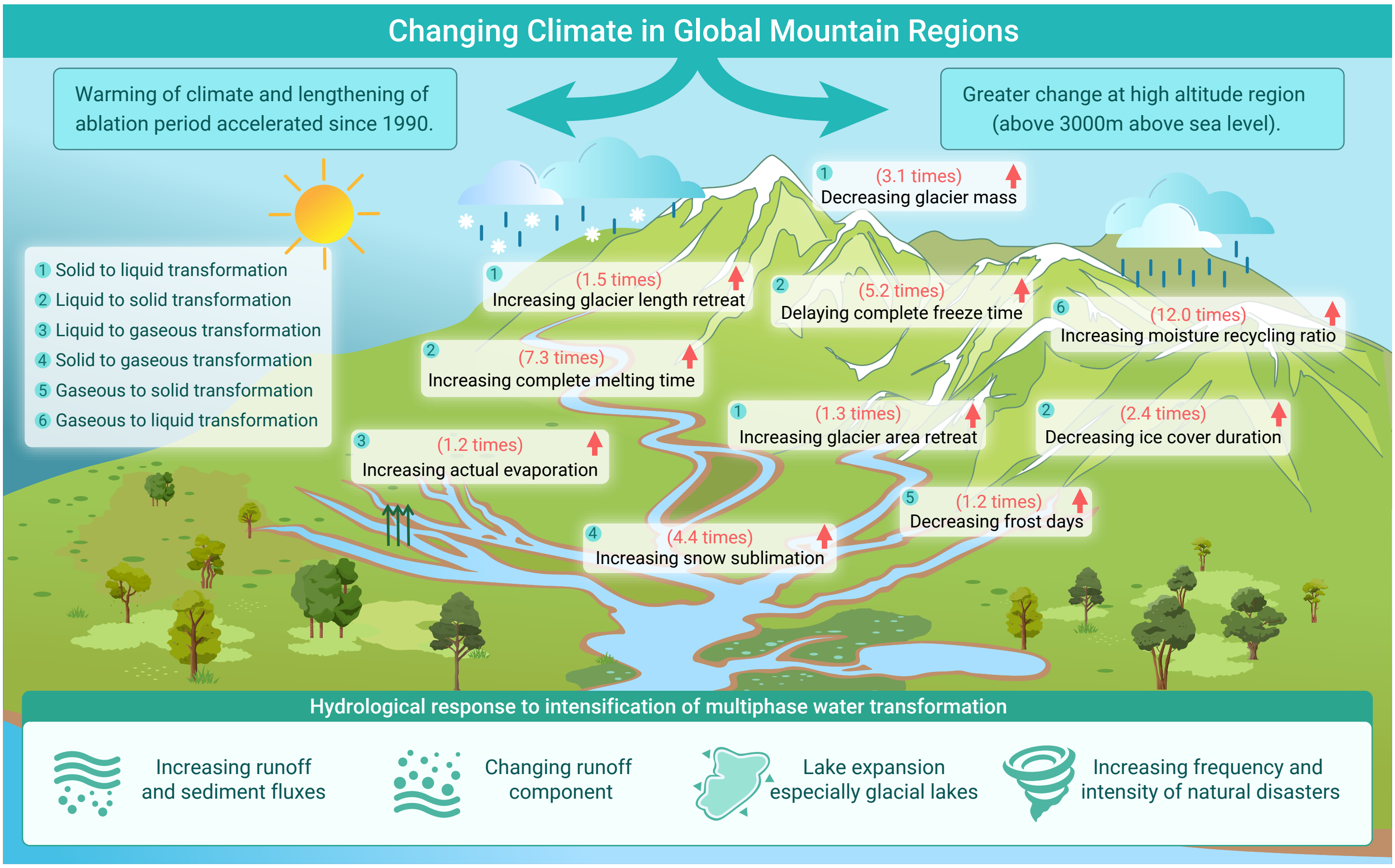

PUBLIC SUMMARY

- Accelerated warming and lengthening ablation period since 1990s strengthened multiphase water transformation (MWT).
- Warming and ablation period indices were higher in 1991–2017 than in 1960–1990.
- Warming trends were greater in high-altitude regions than low-altitude regions.

Accelerated multiphase water transformation in global mountain regions since 1990

Zongxing Li,[1,2] Qi Feng,[1,2] Xufeng Wang,[1,2] Zongjie Li,[3,*] Q J Wang,[4] Deliang Chen,[5,*] Baijuan Zhang,[1,2] and Juan Gui[1,2]

[1]National Key Laboratory of Ecological Security and Sustainable Development in Arid Region/Gansu Qilian Mountains Eco-Environment Research Center, Northwest Institute of Eco-Environment and Resources, Chinese Academy of Sciences, Lanzhou 730000, China

[2]Observation and Research Station of Eco-Hydrology and National Park by Stable Isotope Tracing in Tibetan Plateau, Northwest Institute of Eco-Environment and Resources, Chinese Academy of Sciences, Lanzhou 730000, China

[3]College of Energy and Power Engineering, Lanzhou University of Technology, Lanzhou 730050, China

[4]Department of Infrastructure Engineering, University of Melbourne, Victoria 3010, Australia

[5]Department of Earth Sciences, University of Gothenburg, Gothenburg 40530, Sweden

*Correspondence: lzjie314@163.com (Z.L.); deliang@gvc.gu.se (D.C.)

Received: July 15, 2023; Accepted: November 8, 2023; Published Online: November 15, 2023; https://doi.org/10.59717/j.xinn-geo.2023.100033

Citation: Li Z., Feng Q., Wang X., et al., (2023). Accelerated multiphase water transformation in global mountain regions since 1990. The Innovation Geoscience 1(3), 100033.

Mountains are sensitive to climate change, and while amplified warming at high elevations is widely observed and fairly well understood, changes in the water cycles of mountain regions remain poorly quantified. Due to low temperatures at higher elevations, these changes involve multiphase water transformation (MWT). Through analyzing extensive data from global mountain regions, we determined that under the accelerating warming and lengthening ablation period since the 1990s, the strengthening solid–liquid transformation can be confirmed for 45 glacier basins or single glaciers. This is marked by an increase of 21.5 km^2/10a in glacier area retreat rate, 387.65 mm for average negative glacier mass balance, and 60 m/10a for average glacier length retreat rate (of 414 glaciers) from the study period before the 1990s until the period after the 1990s. The accelerating liquid–solid transformation was indicated by an increase of 31.2 d/10a for the delaying trend of complete freeze time, an increase of 4.3 d/10a for the advancing trend of complete melting time, and an increase of 3.9 d/10a for the decreasing trend of ice cover duration for 22 lakes from the period before the 1990s until the period after the 1990s. The accelerating liquid–gas transformation can be confirmed by an increase of 1 and 0.69 mm/d/10a in the variation trend of actual evaporation and bare-soil evaporation from 1980–1990 to 1990–2017, respectively. Snow sublimation decreased by 0.69 mm/d/10a during 1980–1990, followed by a statistically significant increase of 1.66 mm/d/10a during 1990–2017, further confirming the accelerating solid–gas transformation. The accelerating gas–solid transformation can be reflected by an increase of 0.3 d/10a for the decreasing trend of frost days from 1960–1990 to 1990–2017. The moisture recycling ratio decreased by –0.042 %/10a during 1980–1990 and then increased by 0.443 %/10a during 1990–2017, with the corresponding average values of 12.3% and 13.6%, respectively, which indicates an accelerating gas–liquid transformation. Approximately 59 rivers displayed an increase of 108.60 m^3/s/10a for the runoff variation trend from the period before the 1990s until the period after the 1990s. In addition, the trends for lake number and lake area in the Tibetan Plateau increased 3.86 and 5.75 times, respectively, from 1976–1995 to 1995–2019. This acceleration can significantly change the spatiotemporal pattern of water resources and increase the frequency and intensity of disaster events, such as glacial lake outbursts, flooding, and waterlogging. Consequently, most mountain regions will require strong adaptation efforts to sustain water, food, and ecological security.

INTRODUCTION

The global hydrological cycle is a key component of Earth's climate system; it is also the main form of redistribution of energy on Earth. Understanding and quantifying the observed global water cycle changes is crucial for predicting the future climate. It is widely recognized that the warming of the global surface and lower atmosphere will strengthen the water cycle,[1-3] resulting in changes in water resource availability, frequency and intensity of floods and droughts, and amplification of warming through water vapor feedback and ecosystem services. An intensified global water cycle at a rate of 8 ± 5% per degree of surface warming was observed for the period 1950–2000 based on the global surface salinity changes.[4] A water cycle amplification of 3.0 ± 1.6% /°C was further observed for the period 1950–2010 based on full depth salinity measurements.[5] In addition, the enhanced atmospheric hydrological cycle in the Southern Ocean associated with the warming in the second half of the 20th century resulted in an increase in the Antarctic sea ice over the past three decades.[6] It was also found that the acceleration of global water storage increased to 12 mm/a in regions such as Australia, Turkey, and Northern India over the 2003–2012 period with inter-annual and decadal climate variability.

Satellite observations have revealed that continental evaporation increased at rates consistent with expectations derived from temperature trends dominated by the El Niño–Southern Oscillation.[7] The increasing intensity of the hydrologic cycle can also be proven by an increase of 5400 km^3/10a in global freshwater discharge attributed to an increase in global ocean evaporation (768 0km^3/10a) in the period 1994–2006.[8] The global annual evapotranspiration increased on average by 7.16 mm/a/10a from 1982 to 1997, after which the increase seemingly ceased until 2008 owing to decreasing soil-moisture.[9] Observations from various countries in the Northern Hemisphere showed that pan-evaporation has been steadily decreasing over the past 50 years, contrary to the expectations that the warming would cause increased evaporation.[10-13] Therefore, the evidence for the hydrological cycle accelerating due to variations in evaporation has not been determined yet. Some studies have linked the recent global warming with increasing evaporation; whereas others have reported a decrease in pan-evaporation. However, a direct observational evidence of a positive trend in the global evapotranspiration is still lacking.[14]

Understanding the observed changes in the acceleration of the global water cycle is crucial for predicting future climate changes and their impacts. While many datasets document crucial variables such as precipitation, ocean salinity, runoff, and humidity, most showed significant uncertainties related to determining long-term changes. Furthermore, the in-situ networks provided long time series over land but were sparse in many areas, particularly in mountainous regions. Satellite and reanalysis datasets provided global coverage, but their long-term stability was lacking. Therefore, the acceleration or intensification of the hydrological cycle with global warming is a long-standing paradigm in climate research, and the hypothesis that the water cycle has strengthened on a global land scale requires more evidence. Mountains are extremely important components of the Earth's surface. Although they occupy only about one-eighth of the world's land surface outside Antarctica, they are home to 10% of the world's population, and more than half of the global population is directly or indirectly dependent on mountain resources and services. Mountainous areas are often described as the world's "water towers;" they supply approximately 70% of the world's land freshwater resources.[15] Mountain and hillside areas account for approximately one-third of the habitat for all terrestrial plant and animal species, providing a global barrier for ecological security and the focus areas for global biodiversity conservation. Mountains are also fragile environments that are sensitive to climatic changes; they are highly vulnerable to human and natural ecological imbalances.[16] Under persistent warming, mountain disasters are expected to become increasingly more frequent with a growing list of

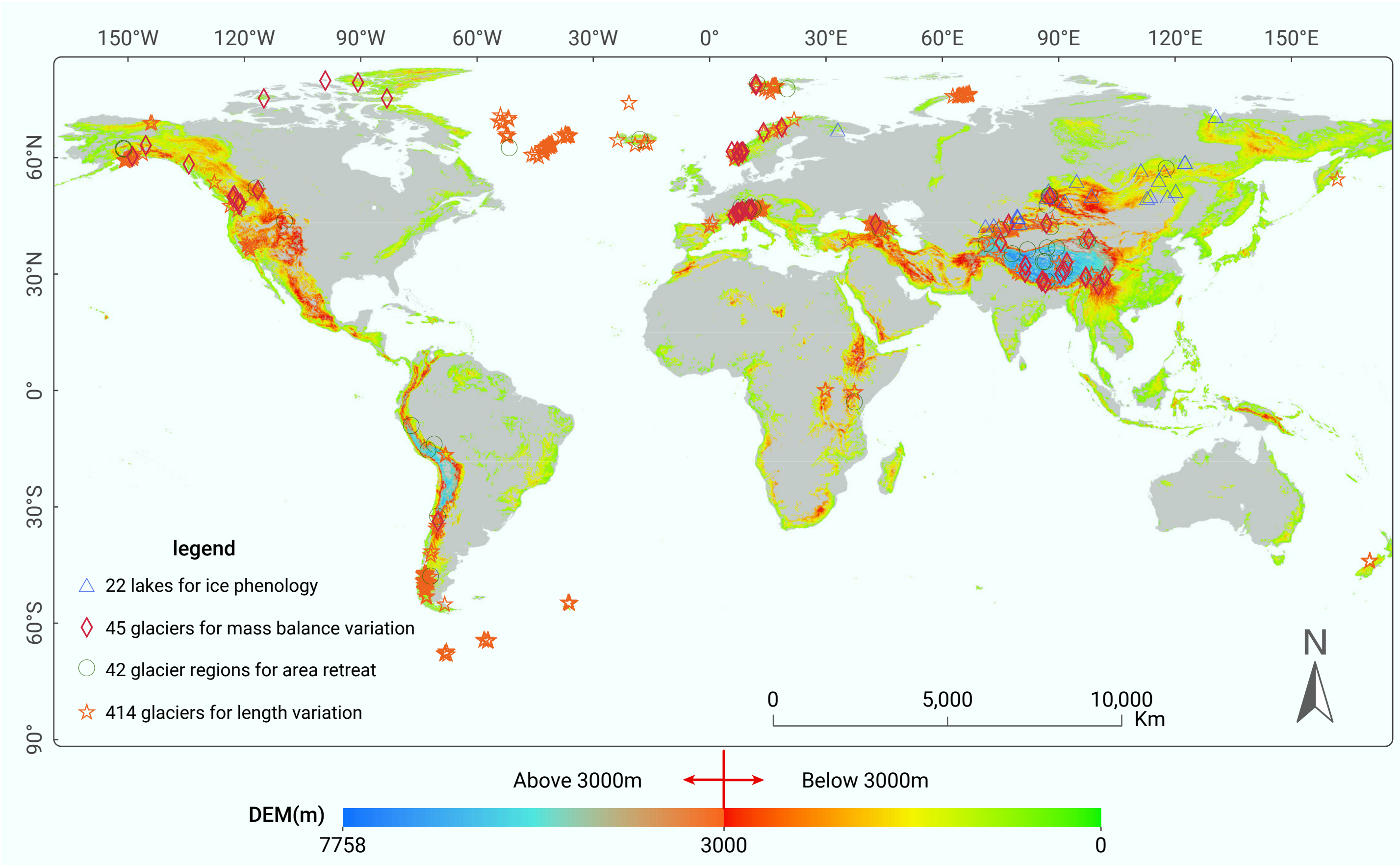

Figure 1. Global mountainous region: above and below 3000 m Above Sea Level (m) spatial distribution of 42 glacier regions for area retreat, 45 glaciers for mass balance variation, 414 glaciers for glacier length retreat, and 22 lakes for ice phenology in the global mountain regions

environmental threats to humans, including floods, landslides, glacial lake bursts, mudrock flows, avalanches, and fires.[17] The hydrological processes in mountain regions are core indicators of the global water cycle. The prominent hydrological features of mountainous regions can be characterized by the coexistence of multiphase waters and their transformations (Figure 1). This refers to the frequent conversions of bodies of water between solid (glaciers, snow cover, lake ice, and permafrost ground ice), liquid (rivers, lakes, marshes, soil water, plant water, and groundwater), and gas (local evapotranspiration vapor and advection vapor) states.[17] Drastic multiphase water transformation (MWT) associated with climate warming has been occurring in the mountain regions comprising glaciers, snow, permafrost, lakes, and vegetation, which are crucial links in the water cycle. The MWT has greatly affected the spatiotemporal patterns of water resources, ecology, and the occurrence of natural disasters, resulting in subsequent social effects.[16-18] However, the possible MWT changes and hydrological responses are poorly understood because of high meteorological variability, physical inaccessibility, and complex interplay between climate, cryosphere, and hydrological processes. Thus, a comprehensive study of MWT is urgently needed to provide a scientific foundation for predicting future water resources, ecological protection, disaster prevention, and risk management. It is important to examine the changes in hydrology in the context of climate change over the global mountain regions to understand the links between the MWT changes and hydrological responses and to develop a sustainable water resource strategy.

Therefore, based on extensive existing data (details regarding the data sources are shown in Support Information), in this review, climate driving for the MWT was analyzed for the global mountainous regions, using the year 1990 as the change point to divide the time series into two periods. The MWT processes related to changes in glacier and permafrost properties, snowfall, evapotranspiration, snow sublimation, lake ice phenology, frost days, and precipitation moisture recycling ratio have been explored in detail. Finally, changes in hydrological processes have also been discussed. This analysis is expected to provide a broad understanding of the frequency, intensity, and duration of MWTs and their hydrological effects. Understanding the potential additive and interactive effects of MWTs on hydrological processes is key to predicting and mitigating the consequences of climate warming in global mountain regions. Finally, we also discuss an increase in the frequency and intensity of natural disasters under MWT. In addition, the study also develops a new theoretical basis, approach, and direction for cold region hydrology.

RESULTS

Intensification of multiphase water transformation since 1960

Solid to liquid transformation. To quantify the intensification of multiphase water transformation during different periods, the variations in glacier areas for 45 glacier regions in the global mountainous regions (Alaska, western North America, northern Canadian Arctic North, southern Canadian Arctic, Iceland, Svalbard and Jan Mayen, Scandinavia, northern Asia, central Europe, central Asia, southwestern Asia, southeastern Asia, low-latitude regions, southern Andes, and New Zealand) were reanalyzed from previous literature, as shown in Supplementary Table 1 and Figure 1. The glacier mass balance data for 42 glaciers in the global mountainous regions were provided by the World Glacier Monitoring Service (https://wgms.ch/) (WGMS, 2017). Glacier mass balance data relevant for longer periods for the Hailuogou Glacier and Baishui Glacier No. 1 in China were obtained from Li et al. (2010),[19] while short-term data for the other 17 glaciers in China were acquired from Yao et al. (2015) (Supplementary Table 2 and Figure 1).[20] The glacier length data for 415 glaciers in the global mountainous regions were obtained from previous studies (Supplementary Table 3 and Figure 1).[19,21-23] Glacier melting is the main phase transformation from solid to liquid water, as indicated by the following three facts. The average glacier area retreat rate was about 73.8 $km^2/10a$ for the 42 glacier regions in the global mountain regions during 1960-2010s (Table 1). Notably, the largest glacier areas retreat occurred in High-Mountain Asia, low-latitude regions, southern Andes, and Alaska, whereas a relatively slow retreat occurred in the eastern Pamir, Kalakunlun and Kunlun

Table 1. Changes in multiphase water transformation during different periods

Transformation	Trend	1960-2010s	before1990	after 1990
Solid–liquid	Average glacier area retreat rate (km^2/10a)	73.80	65.20	86.70
	Average negative glacier mass balance (mm)	364	176	552
	Average retreat rate of glacier length (m/10a)	175.5	115.4	175.4
Liquid–solid	Delaying trend of complete freeze time (d/10a)	23.1	7.5	38.7
	Advancing trend of complete melting time (d/10a)	1.7	-0.8	4.2
	Decreasing trend for ice cover duration (d/10a)	4.8	2.8	6.7
Liquid–gaseous	Increasing trend of actual evaporation(mm/10a)	2.6	4.1	5.1
Gaseous–liquid	Increasing trend of local moisture recycling (%/10a)	0.18	-0.04	0.40
Gaseous–solid	Decreasing trend for number of frost day (d/10a)	2.1	1.9	2.2
Solid–gaseous	Decreasing trend for snow sublimation (mm/10a)	0.3	-0.7	1.7

Mountains, Caucasus, and Scandinavia (Supplementary Table 1). The average negative glacier mass balance was 364 mm for 45 glaciers in the global mountain regions during 1960–2010s (Table 1), while only three glaciers had positive glacier mass balance located in Scandinavia (Supplementary Table 2). The mass balance of the glaciers in Alaska, central Europe (Alps), southern Andes, and High-Mountain Asia exhibited a large loss. Moreover, the average retreat rate of glacier length was -175.5m/10a for 414 glaciers during 1960-2010/11 (Table 1), and all glaciers but 14 displayed a retreat in the global mountain regions (Supplementary Table 3).

Liquid to solid transformation. The variation of lake ice phenology reflected the liquid to solid transformation. The data for lake ice phenology was obtained from National Snow & Ice Data Center (http://nsidc.org/data/G01377.html), which contains freeze and thaw/breakup dates as well as other descriptive ice cover data for lakes and rivers in the Northern Hemisphere. This database includes water bodies distributed around the Northern Hemisphere and allows the analysis of broad spatial and long-term temporal patterns. In this study, one lake in Russia, three lakes in Finland, one lake in Switzerland, one lake in Canada, and 17 lakes in America, all of which are in the global mountainous regions are selected for analyzing the period from the 1960s to the 2000s (Supplementary Table 4 and Figure 1). As a sensitive indicator of climate change, the variation of lake ice phenology for 22 lakes reflected the liquid to solid transformation during 1960–2000 (Supplementary Table 4), and the complete freeze time (no liquid water left) was delayed by -23.10 d/10a, whiles the complete melting time was advanced by 1.70 d/10a, and the ice cover duration (liquid water) was also decreased by -4.80 d/10a in global mountainous regions (Table 1).

Liquid to gaseous transformation. The liquid to gas transformation was represented by evapotranspiration. The actual evaporation data in the global mountainous regions were obtained from the Global Land Evaporation Amsterdam Model Version 3.3a (https://www.gleam.eu/) (Miralles et al., 2010; Martens et al., 2016). In this version, evaporation was estimated based on the reanalysis of net radiation and air temperature, satellite and gauged-based precipitation, satellite-based VOD, and soil moisture. The dataset provides global actual evaporation during 1980–2017 with a spatial resolution of 0.25°. The enhanced liquid to gas transformation was confirmed by increased evaporation, and the actual evaporation increased by 2.60 mm/10a, respectively (Table 1).

Gaseous to liquid transformation. The transformation from gaseous to liquid was confirmed by moisture recycling. Precipitation over a land region is derived from two sources: (1) water vapor evaporated within the region and (2) water vapor evaporated outside of the region and later transported into it (Brubaker et al., 1993). Developed through the Copernicus Climate Change Service (C3S), ERA5 is the fifth major global reanalysis product produced by the European Center for Medium-Range Weather Forecasts. ERA5 is currently available for the period 1979 to the present (https://www.ecmwf.int/en/forecasts/datasets/reanalysis-datasets/era5). We used the total precipitation, evaporation, and vertical integral of the divergence of the moisture flux to calculate the precipitation recycling ratio. All reanalysis data were available within a 0.25° latitude × 0.25° longitude grid. The data covered the period from 1980 to 2017.The strengthened transformation from gaseous to liquid was confirmed by the increased moisture recycling ratio (Table 1), which includes contributions from terrestrial evaporation (on the surface of soil and water) and plant transpiration to precipitation, and the contribution rate from moisture recycling to precipitation was increased by 0.18 %/10a during 1980–2017 in global mountainous regions.

Gaseous to solid transformation. The frost phenomenon involves the transformation of water vapor to solid water when the air temperature falls to 0 °C. RClimDex (http://cccma.seos.uvic.ca/ETCCDI/software.shtml) was used to calculate frost days (FD) from the daily temperature data reported by Berkeley Earth. Frost is an adverse weather event of low-energy status, characterized by ice deposited over plants and objects exposed to an open sky condition.[24] The frost phenomenon involves the transformation of water vapor to solid water when the air temperature falls to 0 °C and the lower atmosphere is humid. It can be quantified by the number of frost days owing to the difficulty in determining the amount of frost. The number of frost days decreased by -2.10 d/10a during 1960–2017 in global mountainous regions (Table 1).

Solid to gaseous transformation. Snow sublimation is a phase transformation from solid to gaseous water. The snow sublimation data in the global mountainous regions were obtained from the Global Land Evaporation Amsterdam Model Version 3.3a during 1980–2017 with a spatial resolution of 0.25° (https://www.gleam.eu/).[26-27] Snow sublimation is the loss of water from the snowpack to the atmosphere, which is a phase transformation from solid to gaseous water that directly affects snow accumulation, which in turn affects ecosystem processes, soil moisture, soil porosity, biogeochemical processes, wildfires, and water resources.[28] Snow sublimation had an increasing trend of 0.3 mm/10a during 1980–2017 in global mountain regions (Table 1).

Accelerated intensification of multiphase water transformation since 1990

Glacier melting has accelerated since 1990 (Figure 2), and the average glacier area retreat rate after 1990 is 1.3 times that before 1990, which increased by 21.50 km^2/10a for the 42 glacier regions (Table 1). Specifically, the glacier area retreat rate increased by 25.60 km^2/10a for 37 glacier regions, whereas it decreased by 331 km^2/10a for the other five glacier regions during the same period (Supplementary Table 1). The average negative glacier mass balance after 1990 is 3.1 times that before 1990, and it increased by 376 mm for the 45 glaciers (Table 1). Further, it increased by 388 mm for 44 glaciers from the period before to that after 1990, while only one glacier in Scandinavia decreased by 124 mm during the same period (Supplementary Table 2). The average glacier length retreat rate after 1990 is 1.5 times that before 1990 for 414 glaciers, and it increased by 60 m/10a (1.5 times that before 1990) from before to after 1990 (Table 1). There are three

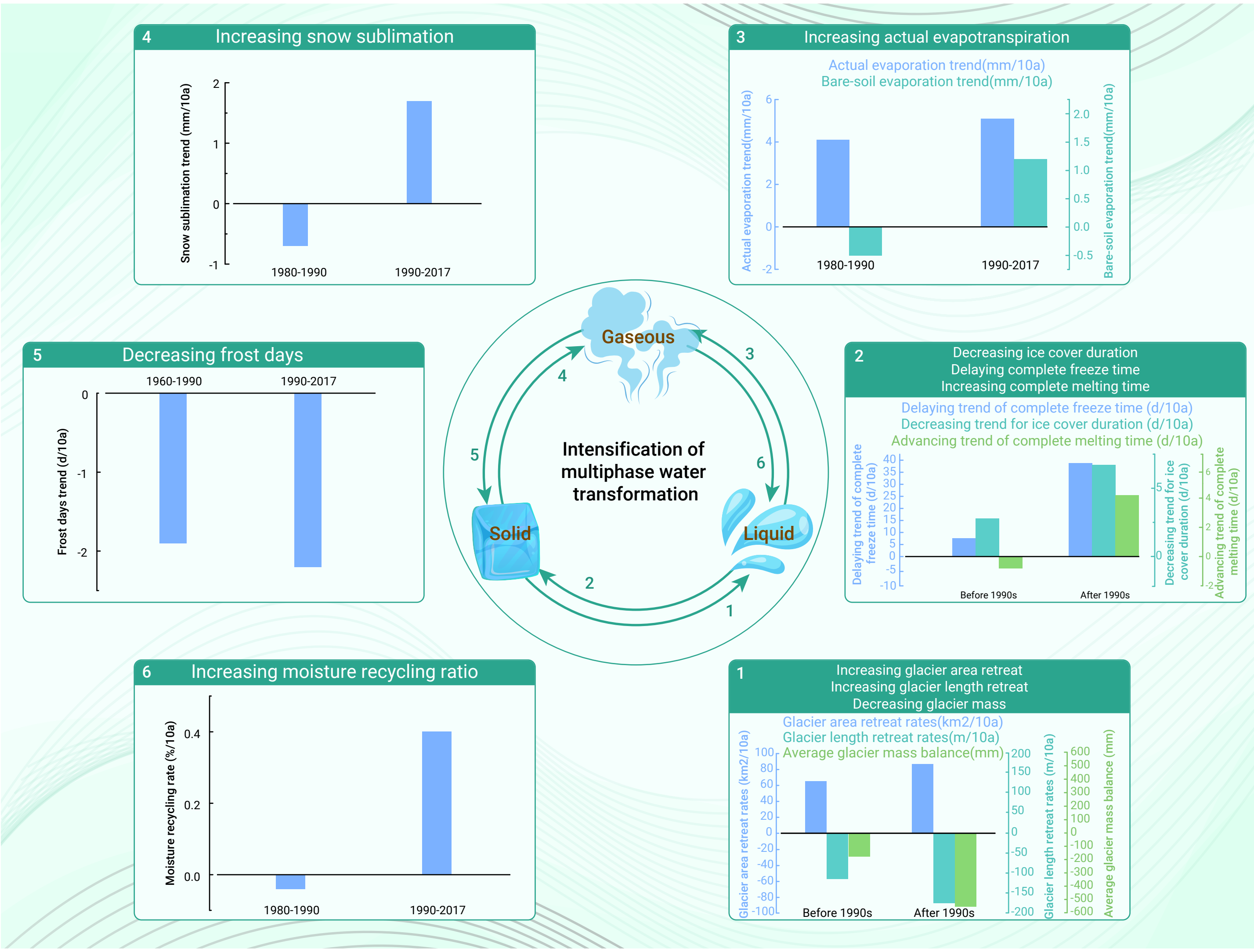

Figure 2. The times for variation rate of MWT after 1990 of that before 1990 in the global mountainous region: ①the enhanced solid to liquid transformation evidenced by 42 glacier regions for area retreat, 45 glaciers for negative mass balance and 414 glaciers for glacier length retreat; ②the reduced liquid to solid transformation reflected by changes in complete freeze time (no liquid water), complete melting time (no ice), and ice cover duration of ice phenology for 22 lakes;③the increased liquid to gas transformation indicated by enhanced actual evaporation; ④the strengthened gaseous to liquid transformation evidenced by the increased moisture recycling ratio, which is defined as the ratio of precipitation contributed by water vapor evaporated within the region to the total precipitation;⑤the reduced gaseous to solid transformation evidenced by decreased number of frost days; ⑥the increased solid to gaseous transformation evidenced by enhanced snow sublimation.

change patterns: firstly, 58 glaciers advanced by 53.10 m/10a before 1990 and then retreated by -139.30 m/10a after 1990; secondly, 227 glaciers retreated at a rate of -115.00 m/10a before 1990 and then retreated by a relatively greater rate of -30.40 m/a after 1990; thirdly, 130 glaciers retreated at a rate of -285 m/10a before 1990 and then retreated at a relatively lower rate of -83 m/10a after 1990 (Supplementary Figure 1, Supplementary Table 3). Moreover, the change in lake ice phenology also accelerated since 1990 in global mountainous regions (Table 1, Supplementary Table 4, Figure 2). The delaying trend of complete freeze time increased by 31.20 d/10a after 1990, to 5.2 times that before 1990. The advancing trend of complete melting time increased by 5 d/10a during the same period (7.3 times that before 1990). The decreasing trend for ice cover duration also increased by 3.90 d/10a during the same period (2.4 times that before 1990). Meanwhile, the increasing evaporation rate has also accelerated since 1990 (Table 1), and the variation trend of actual evaporation increased by 1 mm/10a after 1990, or 1.2 times that before 1990 (Figure 2). More importantly, the contribution ratio from moisture recycling to precipitation increased by 0.4 %/10a during 1991–2017 (Table 1) to 12.0 times that before 1990 (Figure 2). Furthermore, the decreasing trend for frost days also increased by 0.3 d/10a after 1990 (Table 1), to 1.2 times that before 1990 (Figure 2). Finally, changes in snow sublimation also accelerated, and the trend increased to 2.40 mm/10a after 1990 (Table 1), which is 4.4 times that before 1990 (Figure 2).

Drivers for the accelerated intensification

The accelerated intensification of the water cycle since 1990 was mainly caused by the accelerated warming in the global mountainous regions (Figure 3a, b), as demonstrated by the following data. Firstly, the warming magnitudes were 0.16, 0.24, 0.08, 0.05, 0.19, 0.16, and 0.14 °C/10a higher in 1991–2017 than in 1960–1990, for the annual average temperature (TAVG), annual average maximum temperature (TMAX), annual average minimum temperature (TMIN), annual highest daily minimum temperature (TNx), annual lowest daily maximum temperature (TXn), annual highest daily maximum temperature (TXx), and annual lowest daily minimum temperature (TNn) (Figure 3c), respectively. Secondly, the ablation period was also extended in global mountainous regions, and the trends for ice days (ID), cold day frequency (TX10), growing season length (GSL), warm day frequency (TX90) and warm night frequency (TN90) in 1991–2017 were 0.6, 0.9, 0.5, 2 and 1.4d/10a higher than those in 1960–1990, respectively (Figure 3d). Moreover, the warming trends were significantly greater in high-altitude regions (over 3000 m above sea level) than those in in low-altitude regions (below 3000 m above sea level) (Figure 3e, f). Furthermore, the areas with a warming trend accounting for 90%, 82%, 97%, 70%, 63%, 70%, and 68% of the total area in the global mountainous regions during 1960–1990 for TAVG, TMAX, TMIN, TNx, TXn, TXx, and TNn, respectively, increased to 100%, 100%, 100%, 78%, 81%, 80%, and 83% in 1991–2017 (Supplementary Figure 2). In

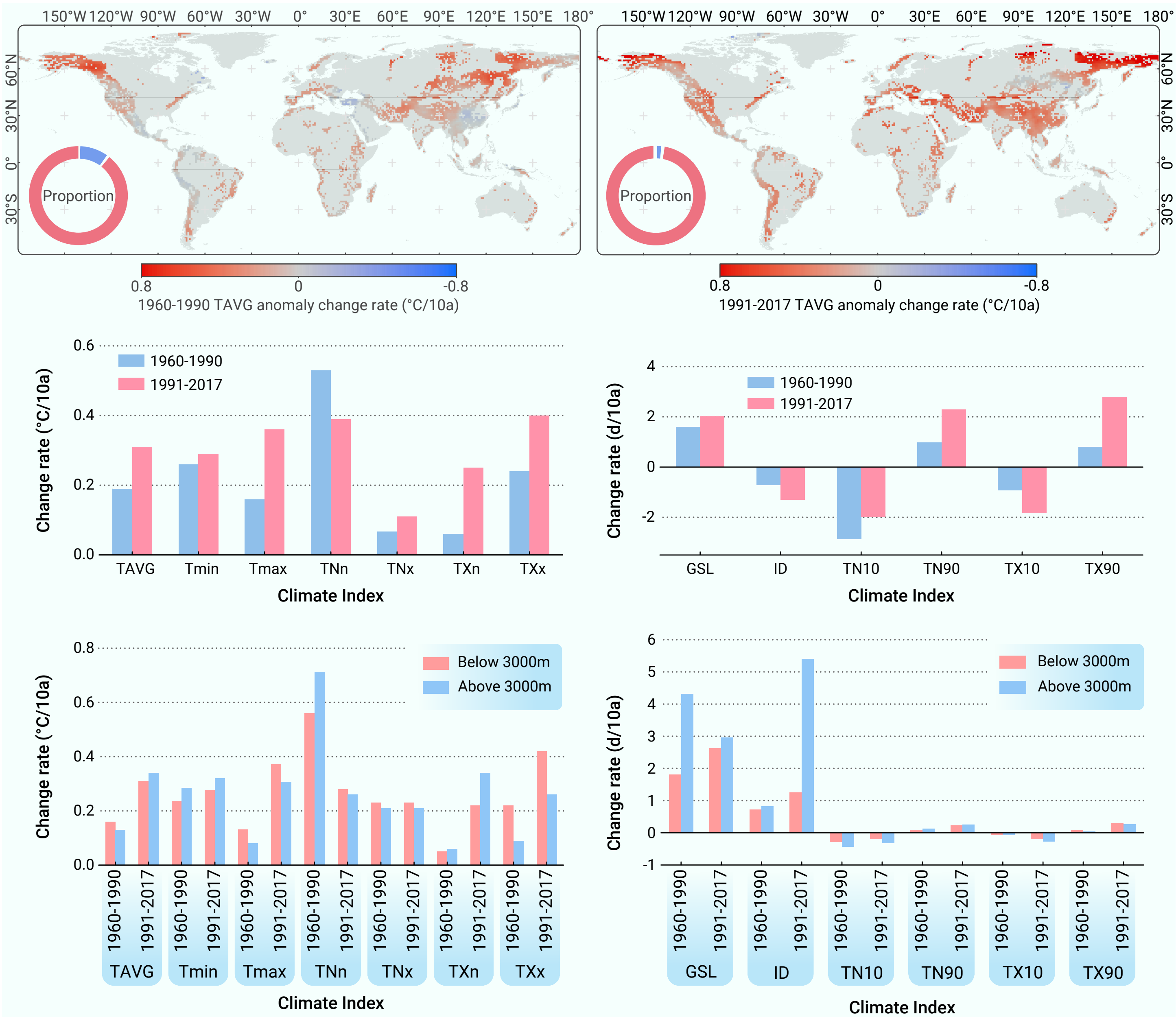

Figure 3. The anomaly change rate of annual average temperature (TAVG) during 1960–1990 (°C/10a) (a), TAVG anomaly change rate during 1991–2017 (°C/10a) (b), warming magnitudes of temperature indices during 1960–1990 and 1990–2017 (°C/10a) (c), warming magnitudes of temperature indices below 3000 m and above 3000 m during 1960–1990 and 1991–2017 (°C/10a) (d), increasing magnitudes of ablation period indices during 1960–1990 and 1991–2017 (d/10a) (e), and increasing magnitudes of ablation period indices below 3000 m and above 3000 m during 1960–1990 and 1991–2017 (d/10a) (f)

addition, during 1960–1990, the areas with extending trends accounted for 42%, 43%, 60%, 93%, 77%, and 84% of the area in the global mountainous regions for ID, GSL, TX10, TN10, TX90, and TN90, respectively, which further increased to 43%, 52%, 90%, 96%, 93%, and 93% during 1991–2017 (Supplementary Figure 3).

IMPLICATIONS

This study has identified an accelerated intensification of the water cycle as evidenced by the accelerating MWT in the global mountainous regions under global warming. Acceleration of the water cycle may lead to not only substantial increases in both runoff and sediment fluxes (Li et al, 2021),[28] and lake, especially glacial lake, expansion,[29-30] but also to changing streamflow patterns, which in turn may exacerbate flooding and water shortages predicted to occur with future climate change.[31-34] For example, (a) the accelerated water cycle would increase the intensity of extreme precipitation events and flooding risks (Tabari, 2020); (b) permafrost degradation would release carbon from thawing permafrost,[35] and reduce the areal extent and duration of wetlands, consequently affecting the carbon cycle;[36] (c) substantial melting of glaciers would result in shifts of seasonal runoff maxima, further decrease summer runoff, and cause water resource scarcity,[37] glacial lake outbursts, and unstable icefalls;[38-40] (d) the removal of glacial ice supporting steep slopes combined with the thawing of permafrost would increase the likelihood of landslides.[41-43] The accelerated MWT could negatively impact and interrupt societal systems (transportation, electrical power, and water provisioning systems), processes (trade, travel, extraction, and shipping), places (residential areas, commercial districts, industrial areas, and recreational sites), and people in risk-prone areas.[44-47] Therefore, most mountainous regions will require strong adaptation efforts to reduce the risk of disasters that can affect developing as well as developed countries under the accelerating MWT.

The findings from this study offer a global systematic assessment and improve our understanding of the acceleration of the water cycle in global mountainous regions. Moreover, the study contributes to a more accessible quantification of the apparent changes in the complex system of the water cycle that will facilitate research into water resource change and its influence. Considering the threat from the acceleration of MWT and the associated future trends in global mountainous regions, we offer the following recommendations: Firstly, an improved in situ monitoring network for MWT is a crucial for predicting the future of the water cycle and associated hazards, including their impacts on regional water, ecosystems, and food security, especially in high-altitude areas (>4000 m) where observations are sparse. Secondly, future research should focus on quantifying the hydrological effects of the accelerating MWT in global mountainous regions, which will elucidate the impacts on the world's "water towers." These changes pose a serious challenge to ecological security, biodiversity patterns, and ecosystem services. Therefore, it is critical to develop scientific strategies to control or reduce potential risks to environmental security under the accelerating MWT. Thirdly, as mountainous areas are typically economically underdeveloped, the international community should work closely with stakeholders to intensify their assistance in building the resilience of mountainous regions, as well as improving disaster prevention capacity and scientific forecasting to address the risks and challenges posed by the accelerating MWT.

Data and materials availability

A 250 m Hammond landform dataset was provided by the United States Geological Survey Land Change Science Global Ecosystems (https://wildfire.cr.usgs.gov/arcgis/rest/services/gmek3/MapServer), which has been used to extract data for the global mountainous regions. The daily gridded land surface temperature dataset from Berkeley Earth was used to examine climate warming trends and to calculate extreme climate indices (http://berkeleyearth.org/data/). The data for glacier areas and glacier lengths were established in this study and were used to calculate the glacier area retreat rates and average retreat rates of glacier lengths (Supplementary Table 1, Supplementary Table 3). The glacier mass balance data for 42 glaciers in global mountainous regions were provided by the World Glacier Monitoring Service (https://wgms.ch/), whereas the data for the other 19 glaciers were collected during this study to calculate the average glacier mass balance during different periods (Supplementary Table 2). The data for lake ice phenology were obtained from the National Snow & Ice Data Center in order to calculate the variation trends (http://nsidc.org/data/G01377.html, Supplementary Table 4). The actual evaporation and snow sublimation data in global mountainous regions were obtained using the Global Land Evaporation Amsterdam Model Version 3.3a for calculating the variation trends (https://www.gleam.eu/). The local moisture recycling ratio was calculated using ERA5 data produced by the European Center for Medium-Range Weather Forecasts (https://www.ecmwf.int/en/forecasts/datasets/reanalysis-datasets/era5).

METHODS

Trends for climate warming and change point detection

The Mann–Kendall trend estimation method[48] was used to detect the linear trend before and after the change point for the variables used in this study, such as climate variables, extreme climate indices, and evaporation. This method has been recommended by the World Meteorological Organization for the trend analysis of meteorological variables. The Mann–Kendall trend test examines nonparametric monotonic trends for time-series data. It is insensitive to outliers and is widely used in climate variable trend testing. The magnitude of the trend was calculated using the Theil–Sen method.[49]

RClimDex (http://cccma.seos.uvic.ca/ETCCDI/software.shtml) was used to calculate climate indices from the daily data reported by Berkeley Earth. The expert team of the Climate Change Detection and Indices coordinated a suite of 11 precipitation and 16 temperature indices adopted by the Intergovernmental Panel on Climate Change Fourth Assessment Report (AR4). A bootstrap procedure was implemented to ensure that percentile-based temperature indices do not have artificial jumps at the boundaries of the base and out-of-base periods.[50] Indices not relevant to the study region were omitted, leading to a final selection of 11 temperature indices: frost days (FD), ice days (ID), TNx (annual highest daily minimum temperature), TXn (annual lowest daily maximum temperature), TXx (annual highest daily maximum temperature), TNn (annual lowest daily minimum temperature), GSL (growing season length), TX10 (cold day frequency), TN10 (cold night frequency), TX90 (warm day frequency), and TN90 (warm night frequency).

The temperature change point was examined using TAVG from the Berkeley Earth data. Considering the uncertainties in change point detection caused by different methods, we chose three widely used methods to detect change points in the TAVG, namely Mann–Kendall method,[48] Pettitt method,[51] Buishand U test, [52] and standard normal homogeneity test (SNHT).[53] The Pettitt and Buishand U test yielded a TAVG change point in 1987, while the SNHT method yielded a TAVG change point in 1993 and the Mann–Kendall method yielded a change point in 1996. Combining the results of the three methods and the length of the data time series, we used the year 1990 as the change point to divide the time series into two periods.

The accelerating intensification of MWT

The solid to liquid transformation. The transformation from solid to liquid water was characterized by the glacier area retreat rate, glacier length retreat rate, and average glacier mass balance. The glacier area retreat rate (Garr) and the accelerating glacier area retreat rate (CGarr) were calculated as follows:

$$\mathrm{Garr} = (\mathrm{A2} - \mathrm{A1})/\mathrm{d} \tag{1}$$

$$\mathrm{CGarr} = \mathrm{Garr2} - \mathrm{Garr1} \tag{2}$$

where A1 and A2 are the glacier areas in the former and latter periods, respectively. Garr1 and Garr2 are the glacier area retreat rate in the former and latter periods, respectively, and d is the number of years between the latter and former periods.

The increasing negative glacier mass balance can be calculated as follows:

$$\mathrm{GMBi} = \mathrm{GMB2} - \mathrm{GMB1} \tag{3}$$

where GMB1 and GMB2 are the glacier mass balances in the former and latter periods, respectively.

The glacier length retreat rate (Glrr) and the accelerating glacier length retreat rate (CGlrr) can be calculated as follows:

$$\mathrm{Glrr} = (\mathrm{A2} - \mathrm{A1})/\mathrm{d} \tag{4}$$

$$\mathrm{CGlrr} = \mathrm{Glarr} - \mathrm{Glrr1} \tag{5}$$

where A1 and A2 are the glacier lengths in the former and latter periods, respectively, and d is the number of years between the latter and former periods.

The liquid to solid transformation. The variation in lake ice phenology for the 22 lakes reflected the accelerating liquid to solid transformation. The variation trend of the complete freeze time, complete melting time, and ice cover duration were calculated using the Mann–Kendall method. In addition, the differential values for the change trends of lake ice phenology before and after 1990 were also calculated.

The liquid to gaseous water, solid to gaseous water, and gaseous to solid water transformations. The accelerating liquid to gas transformation was confirmed by actual evaporation. Snow sublimation is a phase transformation from solid to gaseous water, and frosting is the transformation from gaseous to solid water. Therefore, the variation trends of actual evaporation, snow sublimation, and frost days were also calculated using the Mann–Kendall method, and the differential values for the periods before and after 1990 were calculated.

The gaseous to liquid transformation. The transformation from gaseous to liquid water was confirmed by the moisture recycling ratio, which is defined as the ratio of precipitation contributed by water vapor evaporated within the region to the total precipitation.[54-57] We selected the precipitation recycling ratio calculation model proposed by Van der Ent et al. (2010).[58] The boundaries for the selected global mountainous regions are shown in Figure. 1. The following calculations were performed using MATLAB R2016b software.

Precipitation over a land region was derived from two sources:

$$P(t,x,y) = Pi(t,x,y) + Po(t,x,y) \tag{6}$$

where P_i is the fraction of precipitation from evaporation and P_o is the fraction of moisture flux. The regionally recycled precipitation can be affected by the time (t) and location of the region (x, y).

The precipitation recycling ratio in a region can be expressed as follows:

$$\beta(t,x,y) = \frac{Pi(t,x,y)}{P(t,x,y)} \tag{7}$$

For a certain area Ω, the mass conservation principle can be applied to the water vapor budget.

$$\frac{\partial w''\Omega}{\partial t} = -\nabla \cdot Q''\Omega + E''\Omega - P''\Omega \tag{8}$$

where W_Ω is the precipitable water of a certain area, $\nabla \cdot Q_\Omega$ is the water vapor flux of a certain area, and E_Ω is the evaporation of a certain area.

We assumed that moisture in the atmosphere was well mixed, which implies that:

$$\frac{W''\Omega}{W} = \frac{P''\Omega}{P} \tag{9}$$

By considering only the income of the atmospheric precipitation in this region, the equation can be written as follows:

$$\frac{\mathrm{Wreg}(t,x,y)}{W(t,x,y)} = \frac{E}{-\nabla \cdot Qi + E} \tag{10}$$

where W_{reg} is the precipitable water of a certain area from evaporation. The precipitation recycling ratio in a region can be written as follows:

$$\beta\Omega(\mathrm{year},x,y) = \frac{\sum_{t=1}^{\mathrm{year}}\left[\sum_{(x,y)\in\Omega}\frac{W\Omega(t,x,y)}{W(t,x,y)}P(t,x,y)\right]}{\sum_{t=1}^{\mathrm{year}}\left[\sum_{(x,y)\in\Omega}p(t,x,y)\right]} \tag{11}$$

where β_Ω represents the precipitation recycling ratio in a region.

REFERENCES

1. Allen, M. R., and Ingram. W. (2002). Constraints on future changes in climate and the hydrologic cycle. Nature *419*, 224–232.
2. Helm, K. P., Bindoff, N. L., and Church, J. A. (2010). Changes in the global hydrological-cycle inferred from ocean salinity. Geophys Res Lett. *37*, 1–5.
3. Wentz, F. J., Ricciardulli, L., Hilburn, K., and Mears, C. (2007). How much more rain will global warming bring. Science *317*, 233–235.
4. Durack, P. J., Wijffels S. E., and Matear, R. J. (2012). Ocean salinities reveal strong global water cycle intensification during 1950 to 2000. Science *336*, 455–458.
5. Skliris, N., Zika, J. D., and Nurser, G. (2016). Global water cycle amplifying at less than the Clausius-Clapeyron rate. Sci Rep. *6*, 38752.
6. Liu, J., and Curry, J. A. (2010). Accelerated warming of the Southern Ocean and its impacts on the hydrological cycle and sea ice. P Nat Aca Sci. *107*, 14987–14992.
7. Miralles, D. G., van den Berg, M. J., Gash, J. H., et al. (2014). El Niño–La Niña cycle and recent trends in continental evaporation. Nat Clim Change. *4*, 122–126.
8. Tajdarul, H., Syed, J. S., Famigliettia, D. P. et al. (2010). Satellite-based global-ocean mass balance estimates of interannual variability and emerging trends in continental freshwater discharge. P Nat Aca Sci. *107*, 1–6.
9. Jung, M., Reichstein, M., Ciais, P., et al. (2010). Recent decline in the global land evapotranspiration trend due to limited moisture supply. Nature *467*, 951–954.
10. Peterson, T. C., Golubev, V. S., and Groisman, P. V. (1995). Evaporation losing its strength. Nature *377*, 687–688.
11. Chattopadhyay, N., and Hulme, M. (1997). Evaporation and potential evapotranspiration in India under conditions of recent and future climate change. Agr Forest Meteorol. *87*, 55–73.
12. Thomas, A. (2000). Spatial and temporal characteristics of potential ET trends over China. Inter J Climatol. *20*, 381–396.
13. Ohmura, A., and Wild, M. (2002). Is the hydrological cycle accelerating. Science *298*, 1345–1346.
14. Huntington, T. G. (2006). Evidence for intensification of the global water cycle: review and synthesis. J Hydrol. *319*, 83–95.
15. Brun, F., Berthier, E., Wagnon, P., et al. (2017). A spatially resolved estimate of High Mountain Asia glacier mass balances from 2000 to 2016. Nat Geosci. *10*, 668–673.
16. Nogués-Bravo, D., Araújo, M.B., Errea, M.P., and Martínez-Rica J.P. (2007). Exposure of global mountain systems to climate warming during the 21st Century. Global Environmental Change. *17*, 420–428.
17. Li, Z. X., Feng, Q., Li, Z. J., et al. (2019). Climate background, fact and hydrological effect of multiphase water transformation in cold regions of the western China: A review. Earth-Sci Rev. *190*, 33–57.
18. Li, Z. X., Yuan, R. F., Feng, Q., et al. (2019). Climate background, relative rate, and runoff effect of multiphase water transformation in qilian mountains, the third pole region. Sci Total Environ. *663*, 315–328.
19. Li, Z. X., He, Y. Q., Yang, X. M., et al. (2010). Changes of the Hailuogou glacier, Mt. Gongga, China, against the background of climate change during the Holocene. Quater Int. *218*, 166–175.
20. Yao, T. D., Thompson, L., Yang, W., et al. (2012). Different glacier status with atmospheric circulations in Tibetan Plateau and surroundings. Nat Clim Change. *2*, 663–667.
21. Wang, P. Y., Li Z. Q., Li, H. L., et al. (2014). Comparison of glaciological and geodetic mass balance at Urumqi Glacier No. 1, Tian Shan, Central Asia. Global Planet Change *114*, 14-22.
22. Leclercq, P.W., and Oerlemans, J. (2011). Global and hemispheric temperature reconstruction from glacier length fluctuations. Clim Dynam. *38*, 1065–1079.
23. Leclercq, P. W., Oerlemans, J., Basagic, H. J., et al. (2014). A data set of worldwide glacier length fluctuations. Cryosphere D. *8*, 659–672.
24. Mota, F. S. D. (1983). Meteorologia agrícola. 7. ed. São Paulo: Nobel, 376 p.
25. Martens, B., Miralles, D.G., Lievens, H. (2016). GLEAM v3: satellite-based land evaporation and root-zone soil moisture. Geosci Model Dev. *10*, 1903–1925.
26. Miralles, D. G., Holmes, T. R. H., and De, J. R. A. M., et al. (2010). Global land-surface evaporation estimated from satellite-based observations. Hydrol Earth Syst Sc. *7*, 453–469.
27. Broxton, P. D., Harpold, A. A., Biederman, J. A., et al. (2014). Quantifying the effects of vegetation structure on snow accumulation and ablation in mixed-conifer forests. Ecohydrology *8*, 1073–1094.
28. Li, D. F., Lu, X. X., Overeem, I., et al. (2021). Exceptional increases in fluvial sediment fluxes in a warmer and wetter High Mountain Asia. Science *374*, 599–603.
29. Shugar, D. H., Burr, A., Haritashya, U. K., et al. (2020). Rapid worldwide growth of glacial lakes since 1990. Nat Clim Change. *10*, 939–945.
30. Zhang, G. Q., Luo, W., Chen, W. F., and Zheng, G. X. (2019). A robust but variable lake expansion on the Tibetan Plateau. Sci Bull. *64*, 1306–1309.
31. Blöchl, G., Hall, J., Parajka, J., et al. (2017). Changing climate shifts timing of European floods. Science *357*, 588–590.
32. Papathoma-Köhle, M., Schlögl, M., and Fuchs, S. (2019). Vulnerability indicators for natural hazards: an innovative selection and weighting approach. Sci Rep. *9*, 272–288.
33. Nie, Y., Pritchard, H. D., Liu, Q., et al. (2021). Glacial change and hydrological implications in the Himalaya and Karakoram. Nat Rev Earth Environ. *2*, 91–106.
34. Winsemius, H. C., Aerts, J. C. J. H., van Beek, L. P. H., et al. (2016). Global drivers of future river flood risk. Nat Clim Change. *6*, 381–385.
35. Ding, J. Z., Chen, L. Y., Ji, C. J., et al. (2017). Decadal soil carbon accumulation across Tibetan permafrost regions. Nat Geosci. *10*, 420–425.
36. Avis, C. A., Weaver, A. J., and Meissner, K. J. (2011). Reduction in areal extent of high-latitude wetlands in response to permafrost thaw. Nat Geosci. *4*, 444–448.
37. Sorg, A., Bolch, T., Stoffel, M., et al. (2012). Climate change impacts on glaciers and runoff in Tien Shan (Central Asia). Nat Clim Change. *2*, 725–731.
38. Richardson, S. D., and Reynolds, J. M. (2000). An overview of glacial hazards in the Himalayas. Quatern Int. *65*, 31–47.
39. Cook, K. L., Andermann, C., Gimbert, F., et al. (2018). Glacial lake outburst floods as drivers of fluvial erosion in the Himalaya. Science *362*, 53–57.
40. Osti, R., and Egashira, S. j. (2009). Hydrodynamic characteristics of the Tam Pokhari Glacial Lake outburst flood in the Mt. Everest region, Nepal. Hydrol Process *23*, 2943–2955.
41. Coe, J. A., Bessette-Kirton, E. K., and Geertsema, M. (2018). Increasing rock-avalanche size and mobility in Glacier Bay National Park and Preserve, Alaska detected from 1984 to 2016 Landsat imagery. Landslides *15*, 393–407.
42. Kos, A., Amann, F., Strozzi, T., et al. (2016). Contemporary glacier retreat triggers a rapid landslide response, Great Aletsch Glacier, Switzerland. Geophys Res Lett. *43*, 12466–12474.
43. Liu, J., Wu, Y. M., and Gao, X. (2021). Increase in occurrence of large glacier-related landslides in the high mountains of Asia. Sci Rep. *11*, 1–12.
44. Hungr, O., Evans, S. G., and Hazzard, J. (1999). Magnitude and frequency of rock falls and rock slides along the main transportation corridors of southwestern British Columbia. Can Geotech J. *36*, 224–238.
45. Milly, P. C. D., Wetherald, R. T., Dunne, K. A., and Delworth, T. L. (2002). Increasing risk of great floods in a changing climate. Nature *415*, 514–517.
46. Gariano, S. L., and Guzzetti, F. (2016). Landslides in a changing climate. Earth-Sci Rev. *162*, 227–252.
47. Statham, G., Haegeli, P., Greene, E., et al. (2018). A conceptual model of avalanche hazard. Nat Hazards. *90*, 663–691.
48. Mann, H. B. (1945). Nonparametric tests against trend. Econometrica: J econom soc. *13*, 245–259.
49. Sen, Kumar, P. (1968). Estimates of the regression coefficient based on kendall's tau. Pub Americ Statis Associa. *63*, 1379–1389.
50. Zhang, X.B., Hegerl, G., Zwiers, F. W., and Kenyon, J. (2005). Avoiding inhomogeneity in percentile-based indices of temperature extremes. J Clim. *18*, 1641–1651.
51. Pettitt, A. N. (1979). A non - parametric approach to the change - point problem. J Roy Statis Soc. *28*, 126–135.
52. Buishand, T. A. (1982). Some methods for testing the homogeneity of rainfall records, J Hydrol. *58*, 11–27.

53. Vezzoli, R., Pecora, S., Zenoni, E., and Tonelli, F. (2012). Data analysis to detect inhomogeneity, change points, trends in observations: an application to po river discharge extremes. Social Science Electronic Publishing, *138*, doi:10.2139/ssrn.219534.
54. Sellers, W. D. (1976). A Two–Dimensional Global Climatic Model. Monthly Weather Review, *104*, 233–248.
55. Brubaker, K.L., Entehabi, D., and Eagleson, P.S. (1993). Estimation of continental precipitation recycling. J Climate. *6*, 1077–1089.
56. Eltahir, E. A. B., and Bras, R. L. (1994). Precipitation recycling in the Amazon Basin. Q Journal Roy Meteor Soc. *120*, 861–880.
57. Eltahir, E. A. B., and Bras, R. L. (1996). Precipitation recycling. Rev Geophys. *34*, 367–378.
58. Van der Ent, R. J., Savenije, H. H. G., Schaefli, B., and Steele-Dunne, S. C. (2010). Origin and fate of atmospheric moisture over continents. Water Resour Res. *46*, 1–12.

ACKNOWLEDGMENTS

This work was supported by China's funding agencies: the Joint Funds of the National Natural Science Foundation of China (U22A20592), The "Western Light"–Key Laboratory Cooperative Research Cross-Team Project of Chinese Academy of Sciences, National Nature Science Foundation of China (42367010; 42077187;42107063), Chinese Academy of Sciences Young Crossover Team Project (JCTD-2022-18), National Key Research and Development Program of China (2020YFA0607702), Second Tibetan Plateau Scientific Expedition and Research Program (2019QZKK0405), Innovative Groups in Gansu Province (20JR10RA038), and Swedish Research Council (2021-02163), the Key R&D Plan Projects in Gansu Province(23YFFA0062), The Talent Support Program of Hongliu Youqing in Lanzhou University of Technology. We greatly appreciate suggestions from anonymous referees for the improvement of our paper. Thanks also to the editorial staff.

AUTHOR CONTRIBUTIONS

Zongxing Li designed the research and wrote the paper; Zongxing Li, Qi Feng, Xufeng Wang, Zongjie Li, Deliang Chen performed the research; Q J Wang and Deliang Chen guided the research; Zongjie Li, Baijuan Zhang, Juan Gui analyzed the data.

DECLARATION OF INTERESTS

The authors declare no competing interests.

SUPPLEMENTAL INFORMATION

It can be found online at https://doi.org/10.59717/j.xinn-geo.2023.100033